Assessment of Multicoefficient Correlation Methods, Second-Order Møller–Plesset Perturbation Theory, and Density Functional Theory for H 3 O +(H 2 O) n (n = 1–5) and OH - (H 2 O)...

ARTICLE *in* THE JOURNAL OF PHYSICAL CHEMISTRY B · MARCH 2008

Impact Factor: 3.3 · DOI: 10.1021/jp075823q · Source: PubMed

3 AUTHORS, INCLUDING:

Donald Truhlar
University of Minnesota Twin Cities
1,342 PUBLICATIONS **81,573** CITATIONS

SEE PROFILE

Assessment of Multicoefficient Correlation Methods, Second-Order Møller−Plesset Perturbation Theory, and Density Functional Theory for $H_3O^+(H_2O)_n$ ($n = 1-5$) and $OH^-(H_2O)_n$ ($n = 1-4$)

Erin E. Dahlke, Michelle A. Orthmeyer, and Donald G. Truhlar*

Department of Chemistry and Supercomputing Institute, University of Minnesota, Minneapolis, Minnesota 55455-0431

Received: July 24, 2007; In Final Form: October 16, 2007

We have assessed the ability of 52 methods including 15 multicoefficient correlation methods (MCCMs), two complete basis set (CBS) methods, second-order Møller−Plesset perturbation theory (MP2) with 5 basis sets, the popular B3LYP hybrid functional with 6 basis sets, and 24 combinations of local density functional and basis set to accurately reproduce reaction energies obtained at the Weizmann-1 level of theory for hydronium, hydroxide, and pure water clusters. The three best methods overall are BMC-CCSD, G3SX-(MP3), and M06-L/aug-cc-pVTZ. If only microsolvated ion data is included, M06-L/aug-cc-pVTZ is the best method; it has errors only half as large as the other density functionals. The deviations between the three best performing methods are larger for the larger hydronium- and hydroxide-containing clusters, despite a decrease in the average reaction energy, making it impossible to determine which of the three methods is overall the best, so they might be ranked in order of increasing cost, with BMC−CCSD least expensive, followed by M06-L/aug-cc-pVTZ. However, the cost for M06-L will increase more slowly as cluster size increases. This study shows that the M06-L functional is very promising for condensed-phase simulations of the transport of hydronium and hydroxide ions in aqueous solution.

1. Introduction

The mobility of hydronium and hydroxide ions in liquid water and ice is of great interest to the chemical community from a practical standpoint as they play important roles in many biochemical and organic reactions and also from a fundamental standpoint as they exhibit high mobility compared with other ions in aqueous solution.[1] Of the research that has been done on these ions, a majority of the attention has been paid to the transport of protons in water. It is widely believed that proton transport can be explained by the Grotthuss mechanism[2] which involves interconversion between the Eigen cation[3,4] (a trico-ordinated hydronium ion) and the Zundel cation[5] (the excess proton is shared equally between two water molecules), which is driven by statistical fluctuations in the second solvation shell of the hydronium ion. Knowledge of the transport process for hydroxide ions is more limited, although it is believed that the hydroxide ion is initially coordinated to four water molecules and that fluctuations in the first solvation shell cause one of the hydrogen bonds to break; a resulting proton transfer between the hydroxide ion and one of the neighboring water molecules causes migration of the ion, which goes from having a threefold coordination back to having a fourfold coordination.[6]

Interest in studying solvated hydronium and hydroxide clusters goes as far back as 1933 when Bernal and Fowler[1] proposed a theory to explain the high mobility of hydronium and hydroxide ions in water. Since then, there has been a great deal of computational work focused on trying to determine the properties of these ions in small water clusters,[6,7−21] bulk water,[22−34] and ice.[35,36] Most of the work on small clusters has focused on the use of highly accurate wave function theory (WFT) such as coupled cluster theory with single and double excitations[37,38] (CCSD), CCSD with quasipertubative triples[39] (CCSD(T)), or composite methods such as the Gaussian-*n* methods of Pople and co-workers,[40−44] the CBS extrapolated correlation methods of Peterson and co-workers,[45−52] and the multicoefficient correlation methods (MCCMs) of our group[53−60] and Curtiss et al.[61]

Simulations examining the transport of hydronium and hydroxide in liquid water and ice, however, have focused on the use of density functional theory (DFT),[6,22,26,27] analytic potentials,[25,35,36,62] and in some cases Hartree−Fock theory.[32] Recent simulations[63,64] of pure water have shown that the BLYP[65,66] and PBE[67] functionals do not describe pure water well, which leads one to wonder how they perform for other aqueous systems. Given that many of the DFT-based simulations of H_3O^+ and OH^- in water also utilize these functionals,[6,23,26,31] or similar ones,[22,26,27] it is important to determine how well they are able to perform for these systems.

Past work in our group has attempted to assess a variety of density functionals for their use in the simulation of liquid water by carrying out extensive cluster-based studies.[68,69] The benefit of carrying out cluster studies is that the prediction of more approximate, more affordable theories can be directly compared to results from high-level WFT, and the small size of the systems allow for a very diverse database to be used to test a large numbers of functional and basis set combinations in a reasonable amount of time. Bulk simulations utilizing periodic boundary conditions have been limited mostly to the use of LSDA and GGA functionals. (LSDA functionals use only the local spin densities; GGA functionals utilize both the spin densities and their gradients.) However, recent advances[70−79] have begun to allow for the inclusion of Hartee−Fock exchange and kinetic

* Corresponding author.

10.1021/jp075823q CCC: $40.75
Published on Web 02/05/2008

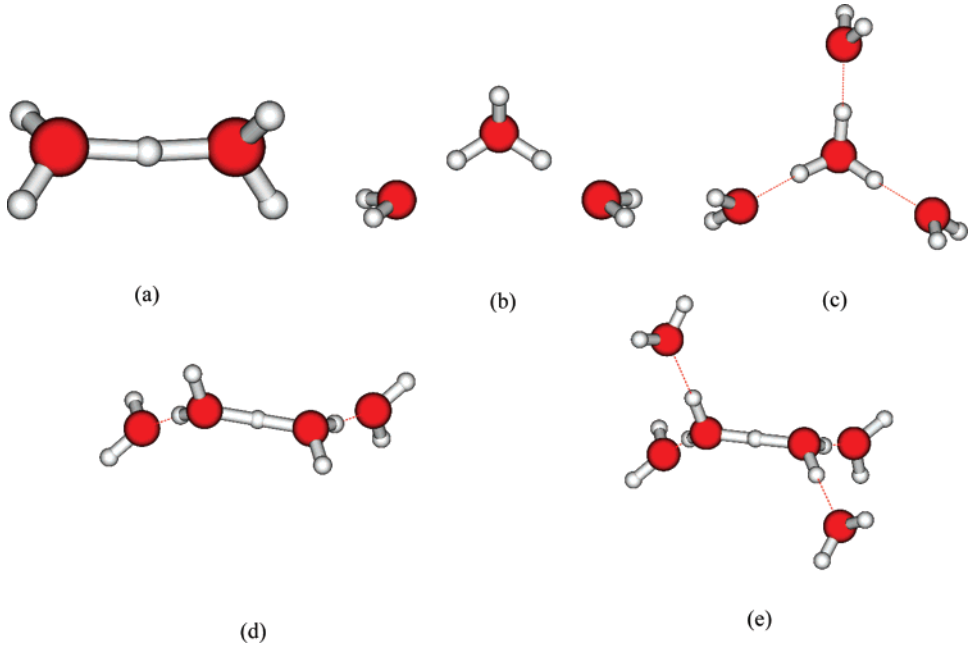

Figure 1. Optimized structures of (a) $H_5O_2^+$, (b) $H_7O_3^+$, (c) $H_9O_4^+$, (d) $H_9O_4^+$(II), and (e) $H_{13}O_6^+$.

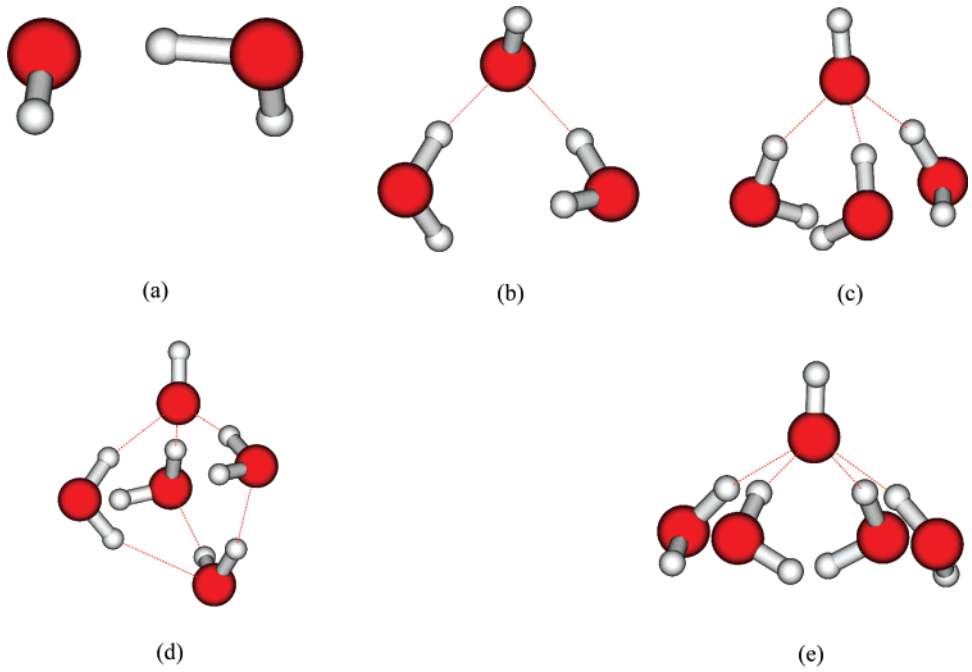

Figure 2. Optimized structures of (a) $H_3O_2^-$, (b) $H_5O_3^-$, (c) $H_7O_4^-$, (d) $H_9O_5^-$, and (e) $H_9O_5^-$(II).

energy density into simulations (hybrid functionals and meta-GGA functionals, respectively; those that include both are called hybrid-meta functionals). This allows for greater flexibility in the choice of functionals; however, the cost of hybrid and hybrid-meta simulations is high (1 to 2 orders of magnitude higher than local functionals[71,76]), and it is useful to have some knowledge of how well a functional will perform for a given system before engaging in a lengthy simulation.

The goal of this paper is to assess the performance of several commonly used functionals for the prediction of accurate energies for a series of hydronium- and hydroxide-containing clusters. In order to do this, we have put together a database of $H_3O^+(H_2O)_n$ (n = 1−5) and $OH^-(H_2O)_n$ (n = 1−4) clusters, for which we will determine accurate electronic energies and use this data to determine which of the density functionals tested is most accurate for the simulation of hydronium and hydroxide ions in water.

2. Databases

In this study, a total of 10 clusters were studied, 5 of which contain hydronuim ions with 1−5 water molecules (see Figure 1) and 5 that contain hydroxide ions with 1−4 water molecules (see Figure 2). For the hydronium-containing clusters, starting structures were taken from Picard et al.[20] for the following structures: $H_5O_2^+$, $H_7O_3^+$, $H_9O_4^+$. Two additional structures ($H_9O_4^+$(II) and $H_{13}O_6^+$) were based on structures from Figure 1 of Kim et al.[13] [denoted $H_9O_4^+$(II) and $H_{13}O_6^+$(II), respectively, in that work]. All structures except $H_{13}O_6^+$ were optimized using quadratic configuration interaction with single and double exciations[80] (QCISD) with the MG3S[81] basis set

TABLE 1: Association Reactions Used in This Study

R1	$H_3O^+ + H_2O \rightarrow H_5O_2^+$
R2	$H_3O^+ + 2H_2O \rightarrow H_7O_3^+$
R3	$H_3O^+ + 3H_2O \rightarrow H_9O_4^+$(II)
R4	$H_5O_2^+ + H_2O \rightarrow H_7O_3^+$
R5	$H_5O_2^+ + 2H_2O \rightarrow H_9O_4^+$(II)
R6	$H_7O_3^+ + H_2O \rightarrow H_9O_4^+$(II)
R7	$OH^- + H_2O \rightarrow H_3O_2^-$
R8	$OH^- + 2H_2O \rightarrow H_5O_3^-$
R9	$OH^- + 3H_2O \rightarrow H_7O_4^-$
R10	$H_3O_2^- + H_2O \rightarrow H_5O_3^-$
R11	$H_3O_2^- + 2H_2O \rightarrow H_7O_4^-$
R12	$H_5O_3^- + H_2O \rightarrow H_7O_4^-$
R13	$H_3O^+ + 3H_2O \rightarrow H_9O_4^+$
R14	$H_5O_2^+ + 2H_2O \rightarrow H_9O_4^+$
R15	$H_7O_3^+ + H_2O \rightarrow H_9O_4^+$
R16	$H_3O^+ + 5H_2O \rightarrow H_{13}O_6^+$
R17	$H_5O_2^+ + 4H_2O \rightarrow H_{13}O_6^+$
R18	$H_7O_3^+ + 3H_2O \rightarrow H_{13}O_6^+$
R19	$H_9O_4^+ + 2H_2O \rightarrow H_{13}O_6^+$
R20	$H_9O_4^+$(II) $+ 2H_2O \rightarrow H_{13}O_6^+$
R21	$OH^- + 4H_2O \rightarrow H_9O_5^-$
R22	$OH^- + 4H_2O \rightarrow H_9O_5^-$(II)
R23	$H_3O_2^- + 3H_2O \rightarrow H_9O_5^-$
R24	$H_3O_2^- + 3H_2O \rightarrow H_9O_5^-$(II)
R25	$H_5O_3^- + 2H_2O \rightarrow H_9O_5^-$
R26	$H_5O_3^- + 2H_2O \rightarrow H_9O_5^-$(II)
R27	$H_7O_4^- + H_2O \rightarrow H_9O_5^-$
R28	$H_7O_4^- + H_2O \rightarrow H_9O_5^-$(II)

[for compounds containing only first and second period atoms (H through Ne) the MG3S basis set is the same as the 6-311+G(2df,2p)[82,83] basis set] level of theory; the $H_{13}O_6^+$ structure was optimized using second-order Møller−Plesset perturbation theory[84] (MP2), also with the MG3S basis set. For the hydroxide-containing clusters, starting structures for $H_3O_2^-$, $H_5O_3^-$, $H_7O_4^-$, and $H_9O_5^-$ were taken from Picard et al.,[20] and one additional structure, referred to as $H_9O_5^-$(II), was based on the 4R4(4 + 0) structure of Figure 1 in Lee et al.[16] All structures except for $H_9O_5^-$ were optimized at the QCISD/MG3S level of theory; the $H_9O_5^-$ structure was optimized at the MP2/MG3S level. Monomer geometries for H_2O, H_3O^+, and OH^- were optimized at the QCISD/MG3S level of theory, for a total of 13 structures. These thirteen structures are given in Supporting Information.

The new cluster data developed in this article to test the different methods consists of 64 reaction energies, which can be broken up into two classes: association reactions and neutralization reactions. Twenty-eight association reactions (R1 to R28) were considered, each involving the addition of one or more water molecules to an ion (hydronium or hydroxide) or ion cluster. The full list of association reactions studied is given in Table 1. The neutralization reactions involve a hydronium ion or cluster reacting with a hydroxide ion or cluster to form water. The 36 neutralization reactions studied are listed in Table 2.

In order to find a method that is accurate for pure water as well as for hydronium- and hydroxide-containing clusters, we also include the Weizmann-1 binding energies, determined in previous work,[68,69] for a representative data set[85] of seven water dimers and trimers (Figure 3), denoted as W7, and a set of six tetramer and one pentamer data (Figure 4). The details of the structures in the W7[68] data set and tetramer and pentamer data[69] are presented in previous work and are not discussed here. The database for which accurate Weizmann-1 energies are known (which consists of the reaction energies for R1 to R12 and R29 to R44, along with the seven binding energies for the W7 representative set and the six tetramer and pentamer clusters) will be referred to in this work as the W42 database because it consists of 42 water data. The accurate Weizmann-1 data for

TABLE 2: Neutralization Reactions Used in This Study

R29	$H_3O^+ + OH^- \rightarrow 2H_2O$
R30	$H_3O^+ + H_3O_2^- \rightarrow 3H_2O$
R31	$H_3O^+ + H_5O_3^- \rightarrow 4H_2O$
R32	$H_3O^+ + H_7O_4^- \rightarrow 5H_2O$
R33	$H_5O_2^+ + OH^- \rightarrow 3H_2O$
R34	$H_5O_2^+ + H_3O_2^- \rightarrow 4H_2O$
R35	$H_5O_2^+ + H_5O_3^- \rightarrow 5H_2O$
R36	$H_5O_2^+ + H_7O_4^- \rightarrow 6H_2O$
R37	$H_7O_3^+ + OH^- \rightarrow 4H_2O$
R38	$H_7O_3^+ + H_3O_2^- \rightarrow 5H_2O$
R39	$H_7O_3^+ + H_5O_3^- \rightarrow 6H_2O$
R40	$H_7O_3^+ + H_7O_4^- \rightarrow 7H_2O$
R41	$H_9O_4^+$(II) $+ OH^- \rightarrow 5H_2O$
R42	$H_9O_4^+$(II) $+ H_3O_2^- \rightarrow 6H_2O$
R43	$H_9O_4^+$(II) $+ H_5O_3^- \rightarrow 7H_2O$
R44	$H_9O_4^+$(II) $+ H_7O_4^- \rightarrow 8H_2O$
R45	$H_9O_4^+ + OH^- \rightarrow 5H_2O$
R46	$H_9O_4^+ + H_3O_2^- \rightarrow 6H_2O$
R47	$H_9O_4^+ + H_5O_3^- \rightarrow 7H_2O$
R48	$H_9O_4^+ + H_7O_4^- \rightarrow 8H_2O$
R49	$H_3O^+ + H_9O_5^- \rightarrow 6H_2O$
R50	$H_3O^+ + H_9O_5^-$(II) $\rightarrow 6H_2O$
R51	$H_5O_2^+ + H_9O_5^- \rightarrow 7H_2O$
R52	$H_5O_2^+ + H_9O_5^-$(II) $\rightarrow 7H_2O$
R53	$H_7O_3^+ + H_9O_5^- \rightarrow 8H_2O$
R54	$H_7O_3^+ + H_9O_5^-$(II) $\rightarrow 8H_2O$
R55	$H_9O_4^+ + H_9O_5^- \rightarrow 9H_2O$
R56	$H_9O_4^+ + H_9O_5^-$(II) $\rightarrow 9H_2O$
R57	$H_9O_4^+$(II) $+ H_9O_5^- \rightarrow 9H_2O$
R58	$H_9O_4^+$(II) $+ H_9O_5^-$(II) $\rightarrow 9H_2O$
R59	$H_{13}O_6^+ + OH^- \rightarrow 7H_2O$
R60	$H_{13}O_6^+ + H_3O_2^- \rightarrow 8H_2O$
R61	$H_{13}O_6^+ + H_5O_3^- \rightarrow 9H_2O$
R62	$H_{13}O_6^+ + H_7O_4^- \rightarrow 10H_2O$
R63	$H_{13}O_6^+ + H_9O_5^- \rightarrow 11H_2O$
R64	$H_{13}O_6^+ + H_9O_5^-$(II) $\rightarrow 11H_2O$

these four types of data can be found in Tables 3 through 6. The database consisting of all of the reaction energies for R1 to R64 and the binding energies for the W7 and tetramer and pentamer data will be called the W78 database because it has 78 data for water. The subset of W42 with only ionic data is called ionic water data set IW28.

3. Computational Methods

Geometries for each of the 13 structures were obtained as described in the previous section. Past work on pure water clusters (up to the water pentamer) has utilized the Weizmann-1[86] (W1) level of theory to determine accurate binding energies against which to test the density functionals. Those works, however, focused primarily on water dimers and trimers, with only a small number of tetramers and a single pentamer calculation. On the basis of the effort required in those works, the application of the Weizmann-1 theory to all 10 of the clusters in this study would be a daunting task, as half of them contain 4 oxygen atoms or more. As a compromise, the Weizmann-1 theory will be used to obtain accurate energies for the three smallest hydronium and hydroxide clusters, as well as H_2O, H_3O^+, and OH^-, and these energies will be used to determine the best possible method for use on the remaining four clusters. The three hydronium-containing clusters calculated at the Weizmann-1 theory are $H_5O_2^+$, $H_7O_3^+$, and $H_9O_4^+$(II). [Since $H_9O_4^+$(II) and $H_9O_4^+$ contain the same number of atoms, $H_9O_4^+$(II) was chosen because it has a higher point group (C_2) than $H_9O_4^+$ (C_1).] Weizmann-1 was also used to obtain accurate energies for the following hydroxide-containing clusters: $H_3O_2^-$, $H_5O_3^-$, and $H_7O_4^-$. With these nine energies in hand, accurate reaction energies can be computed for association reactions R1 to R12 and neutralization reactions R29 to R44.

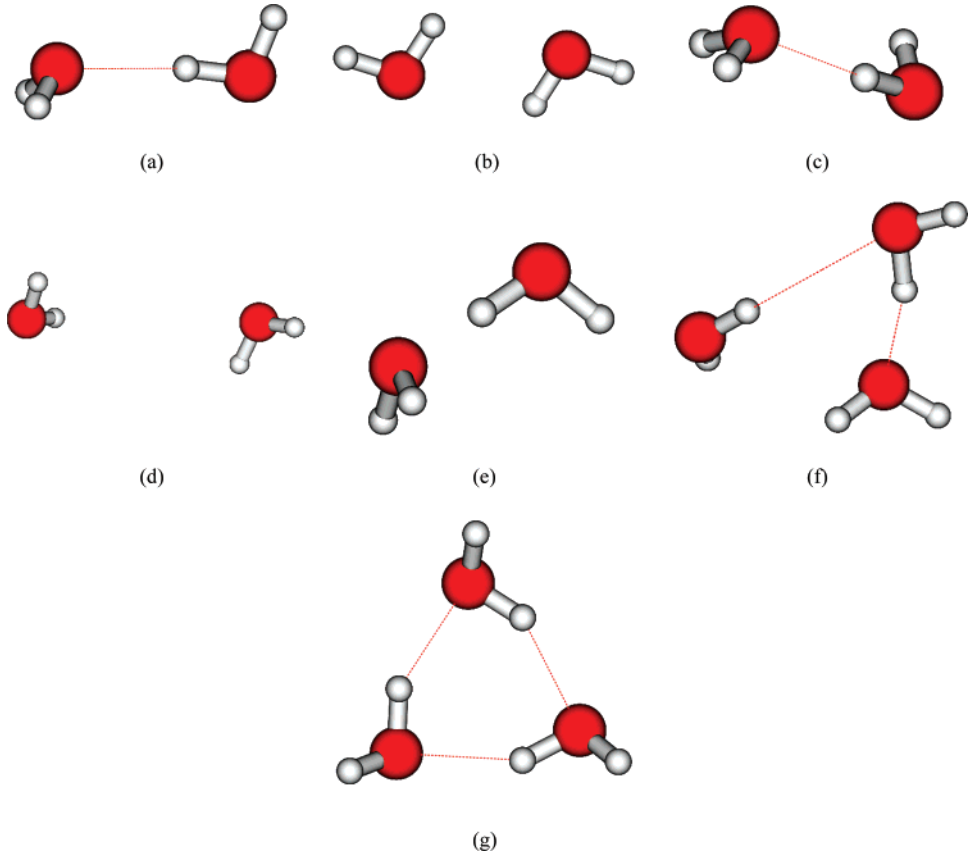

Figure 3. Structures of water dimers and trimers in the W7 database (a) NPOCs, (b) CC2h, (c) dnvt, (d) v523, (e) 50GPa, (f) tnvt, (g) C3LM.

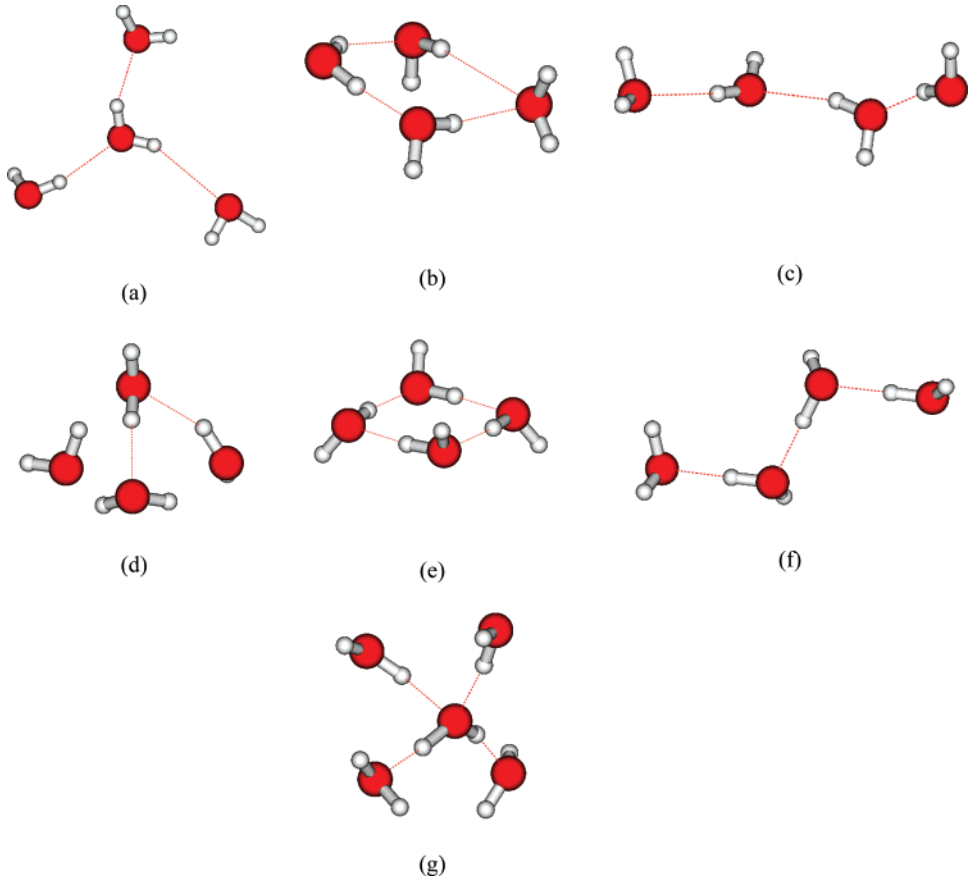

Figure 4. Tetramer and pentamer structures (a) BT, (b) CT, (c) CT, (d) BT2, (e) CT2, (f) LT2, (g) pentamer.

In this work, we test a number of multicoefficient correlation methods (MCCMs). The MCCMs tested in this paper are BMC-CCSD,[85] G3SX,[61] G3SX(MP3),[61] MC3BB,[59] MC3MBWB95,[59] MCG3/3,[58] MCG3-MPWB,[59] MC-QCISD/3,[58] MCG3-MPW,[59]

TABLE 3: Weizmann-1 Reaction Energies (Kilocalories per Mole) for Association Reactions R1 to R12

R1	−33.90
R2	−57.46
R3	−73.18
R4	−23.56
R5	−39.28
R6	−15.72
R7	−26.00
R8	−47.59
R9	−68.10
R10	−21.59
R11	−42.09
R12	−20.51
average	−39.08

TABLE 4: Weizmann-1 Reaction Energies (Kilocalories per Mole) for Neutralization Reactions R29 to R44

R29	−225.95
R30	−199.95
R31	−178.36
R32	−157.85
R33	−192.05
R34	−166.05
R35	−144.46
R36	−123.96
R37	−168.49
R38	−142.49
R39	−120.90
R40	−100.39
R41	−152.77
R42	−126.77
R43	−105.18
R44	−84.67
average	−149.39

TABLE 5: Weizmann-1 Binding Energies[a] (Kilocalories per Mole) for W7 Database

NPOCs	5.00
CC2h	4.00
dimer.nvt	4.60
dimer.vapor.523K	0.10
50GPa	−1.30
trimer.nvt	7.05
C3LM	14.99
average magnitude[b]	5.29

[a] $E_{bind} = E_A + E_B + \cdots + E_N - E_{AB...N}$ where E_A, E_B, etc. are the energy of the unrelaxed monomers and $E_{AB...N}$ is the energy of the cluster containing N water molecules. [b] Average magnitude for this table denotes the average magnitude of the binding energies

MCG3-TS,[59] MCUT/3,[58] MCQCISD-MPW,[59] MCQCISD-TS,[59] MC3MPW,[59] and MCCO/3.[58] On the basis of the work of Picard et al.,[20] we also include single-point CBS-QB3 and CBS-APNO calculations (i.e., we do not carry out the geometry optimization and report only the zero-point-exclusive electronic energy at 0 K). Additionally, since second-order Møller−Plesset perturbation theory (MP2) performs well for small water clusters, we also test MP2 theory with the following basis sets: aug′-cc-pVDZ, aug′-cc-PVTZ, aug′-cc-PVQZ, MG3, and MG3S. The aug′-cc-pVXZ (X = D, T, or Q) basis set denotes the use of the aug-cc-pV*X*Z basis set[87,88] on oxygen and the cc-pVTZ basis set[89] on hydrogen. For the clusters considered in this work, the MG3[81] basis set is the same as the 6-311++(2df,2p),[82,83] and as mentioned previously, the MG3S basis set is the same as the 6-311+G(2df,2p) basis set.

All MCCM calculations were carried out with the MLGAUSS software package,[90] and all MP2 calculations were carried out with *Gaussian 03*.[91]

TABLE 6: Weizmann-1 Binding Energies[a] (Kilocalories per Mole) for Tetramers and Pentamers

BT	10.72
CT	11.55
LT	13.02
BT2	23.57
CT2	28.62
FC	18.31
P	17.84
average	17.66

[a] $E_{bind} = E_A + E_B + \cdots + E_N - E_{AB...N}$ where E_A, E_B, etc. are the energy of the unrelaxed monomers and $E_{AB...N}$ is the energy of the cluster containing N water molecules.

TABLE 7: Basis Set Sizes

basis set	primitive functions[a]	contracted functions[a]
aug-cc-pVTZ	127	92
6-311+G(2df,2p)	74	52
6-311+G(2d,2p)	64	45
aug-cc-pVDZ	65	41
6-31+G(d,2p)	52	35
6-31+G(d,p)	46	29

[a] Per water molecule.

A total of seven density functionals were studied: BLYP,[65,66] B3LYP,[65,66,92,93] PBE,[67] PBE1W,[68] BPW91,[65,94] PBELYP,[66,67] and M06-L.[95] BLYP and PBE were chosen because they are two commonly used[63,64,76,96−101] GGA functionals for the simulation of water and ice, and BLYP has been used[6] in simulations of aqueous OH^-. PBE1W was chosen because it is a variant of the PBE functional that has been parametrized specifically for water. B3LYP was chosen because of its popular use in quantum chemistry and because it has been used[76] for simulating liquid water. Since the focus of this work in on assessing the ability of local functionals to describe these systems, B3LYP is the only nonlocal functional tested. For each of these four functionals, six basis sets were considered: aug-cc-pVDZ, aug-cc-pVTZ, MG3S (6-311+G(2df,2p)), 6-311+G-(2d,2p), 6-31+G(d,2p),[102] and 6-31+G(d,p).[102] These basis sets have been used in the past for evaluating the accuracy of density functionals for small water clusters.[103] The BPW91 and PBE-LYP functionals were chosen because they provide combinations of exchange and correlation functionals utilized in the BLYP, B3LYP, PBE, and PBE1W functionals that may help determine whether it is the exchange or correlation portion of these functionals that most impacts performance. For simplicity the BPW91 and PBELYP functionals are tested only with the 6-311+G(2d,2p) and aug-cc-pVTZ basis sets. Finally, the M06-L density functional was added, which is a meta-GGA that has been shown to have good performance for noncovalent interactions.[95,104] Inclusion of the M06-L functional allows comparison of the methods that are currently being used in simulation to a newer-generation functional that has yet to be used in simulation but which appears to have great promise for a wide variety of applications. The M06-L functional is tested with only the MG3S and aug-cc-pVTZ basis sets. The MG3S and aug-cc-pVTZ basis sets were chosen on the basis of the results of previous work.[95]

All density functional calculations except the M06-L methods were done using *Gaussian 03*. The M06-L calculations were carried out using a locally modified version of *Gaussian 03* (MN-GFM[105]).

In order to provide a context for understanding the performances of the various basis sets, Table 7 gives the number of primitive and contracted Gaussian basis functions per water molecules for each basis studied.

TABLE 8: Mean Unsigned Errors[a] (Kilocalories per Mole) and Timings[b] for the MCCM, MP2, CBS, and DFT Methods

	association (12[c])	neutralization (16)	water (14)	W42 (42)			
	MUE	MUE	MUE	MUE	SA-W42[d]	SA-IW28[e]	timing
BMC-CCSD	0.84	**0.90**[d]	**0.18**	**0.64**	**0.28**	**0.34**	13
G3SX(MP3)	0.85	1.25	0.33	**0.83**	**0.35**	0.38	56
G3SX	0.72	1.24	0.46	**0.83**	0.36	**0.34**	79
MCUT/3	0.95	1.22	0.47	0.89	0.40	0.40	9.0
MC3BB	1.03	0.99	0.58	0.86	0.44	0.40	12
MCG3/3	1.07	0.96	0.57	0.86	0.44	0.41	24
MC-QCISD/3	1.12	1.04	0.60	0.92	0.46	0.43	11
MCG3-TS	1.10	0.99	0.78	0.95	0.51	0.42	30
MCG3-MPW	1.10	1.18	0.75	1.02	0.52	0.44	26
MCQCISD-TS	1.12	**0.95**	0.84	0.96	0.53	0.42	24
MCCO/3	1.32	2.05	0.47	1.32	0.54	0.60	8.8
MCG3/MPWB	1.23	1.18	0.86	1.09	0.57	0.48	28
MCQCISD-MPW	1.16	1.39	0.92	1.17	0.59	0.48	20
MC3MPWB95	1.63	2.59	0.58	1.64	0.66	0.74	12
MC3MPW	2.35	4.17	0.87	2.55	1.00	1.12	9.6
MP2/aug′-cc-pVQZ	**0.62**	3.06	**0.12**	1.39	0.38	0.51	733
MP2/aug′-cc-pVTZ	**0.67**	3.34	**0.10**	1.50	0.40	0.55	58
MP2/aug′-cc-pVDZ	**0.49**	3.77	0.24	1.66	0.44	0.55	2.1
MP2/MG3	1.31	2.51	3.92	2.64	1.58	0.65	10
MP2/MG3S	1.34	2.51	4.44	2.82	1.74	0.65	8.3
CBS-APNO	0.80	1.76	0.20	0.97	**0.34**	0.42	378
CBS-QB3	0.83	1.00	1.75	1.20	0.74	**0.34**	53
B3LYP/6-311+G(2d,2p)	1.32	2.41	0.67	1.52	0.62	0.64	8.5
B3LYP/6-311+G(2df,2p)	1.36	2.45	0.73	1.56	0.65	0.65	14
B3LYP/aug-cc-pVDZ	1.08	3.38	1.15	1.98	0.79	0.67	11
B3LYP/aug-cc-pVTZ	1.10	2.44	1.48	1.74	0.82	0.58	108
B3LYP/6-31+G(d,2p)	2.20	6.01	0.48	3.08	0.99	1.28	3.9
B3LYP/6-31+G(d,p)	3.32	9.40	1.18	4.92	1.66	1.97	2.2
M06-L/aug-cc-pVTZ	0.78	**0.82**	0.47	**0.69**	**0.35**	**0.31**	59
M06-L/6-311+G(2df,2p)	0.94	2.00	0.40	1.17	0.44	0.49	14
PBE1W/6-311+G(2d,2p)	1.98	5.70	0.25	2.82	0.86	1.18	7.2
PBE1W/6-311+G(2df,2p)	2.01	5.69	0.25	2.83	0.87	1.19	14
PBE1W/aug-cc-pVTZ	1.40	6.03	0.96	3.02	0.98	1.05	40
PBE1W/aug-cc-pVDZ	1.64	7.00	0.59	3.33	0.99	1.23	7.6
BLYP/6-311+G(2d,2p)	1.15	3.58	1.95	2.34	1.05	0.72	7.2
BLYP/6-311+G(2df,2p)	1.20	3.61	2.01	2.39	1.08	0.73	14
PBE/aug-cc-pVTZ	2.11	8.37	0.40	3.92	1.12	1.51	40
BLYP/6-31+G(d,2p)	1.76	7.30	1.31	3.72	1.25	1.30	4.2
PBE/aug-cc-pVDZ	2.43	9.31	0.47	4.40	1.27	1.70	9.8
BLYP/aug-cc-pVDZ	1.32	5.08	2.45	3.13	1.34	0.93	9.7
BPW91/6-311+G(2d,2p)	2.01	1.78	2.94	2.23	1.37	0.76	5.3
PBE/6-311+G(2df,2p)	2.86	8.08	0.85	4.18	1.38	1.69	14
PBE/6-311+G(2d,2p)	2.85	8.11	0.92	4.21	1.40	1.69	7.3
BLYP/aug-cc-pVTZ	1.59	3.87	2.80	2.86	1.40	0.87	40
PBE1W/6-31+G(d,2p)	2.90	9.29	0.65	4.58	1.41	1.83	4.6
PBELYP/aug-cc-pVTZ	2.11	10.15	1.05	4.82	1.44	1.71	41
BLYP/6-31+G(d,p)	2.60	10.80	0.75	5.11	1.50	1.91	2.2
PBELYP/6-311+G(2d,2p)	3.06	9.70	1.92	5.21	1.85	1.92	5.8
PBE/6-31+G(d,2p)	3.96	11.70	1.55	6.10	2.05	2.40	4.6
PBE1W/6-31+G(d,p)	4.04	12.78	1.82	6.63	2.23	2.54	2.6
BPW91/aug-cc-pVTZ	5.99	6.06	3.82	5.30	2.69	2.36	53
PBE/6-31+G(d,p)	5.16	15.22	2.80	8.20	2.90	3.12	2.5
average	1.77	4.58	1.14	2.63			

[a] MUE denotes mean unsigned errors. [b] CPU time needed to calculate the reaction $H_7O_3^+ + H_5O_3^- \rightarrow 6H_2O$, relative to the MP2/6-31+G(d,p) level of theory. [c] Number in parentheses denotes total number of reaction energies of that type. [d] SA-W42 denotes the overall scaled average, that is, the one including both the neutral and ionic data. In particular, SA-W42 = ((MUE(association)/(1.77 kcal/mol)) + (MUE(neutralization)/(4.58 kcal/mol)) + (MUE(water)/(1.14 kcal/mol)))/3; note that the scaled average is unitless. [e] SA−IW28 denotes the scaled average for the 28 ionic data only, with the 14 data for pure water clusters removed, that is SA-IW28 = ((MUE(association)/(1.77 kcal/mol)) + (MUE(neutralization)/(4.58 kcal/mol)))/2; note that scaled averages are unitless. [f] The three lowest errors of each type are in bold. There are four bold numbers when there is a tie for third best (all values being rounded to 0.01 kcal/mol)

Single-point energy calculations were carried out on the W42 database with each of the 52 methods (where a method denotes an MCCM or a combination of MP2 or density functional with a basis set), and errors were computed relative to the Weizmann-1 energies. Table 8 shows the mean unsigned errors for all 52 methods. In order to give the reader an idea of how expensive the various methods are, we have calculated the time needed to calculate the reaction energy for neutralization reaction R39 ($H_7O_3^+ + H_5O_3^- \rightarrow 6H_2O$) and have expressed these timings relative to the same calculation at the MP2/6-31+G(d,p) level of theory. The initial purpose of the small database was to test the MCCM, CBS, and MP2 methods in order to find a method that could be used to further test the density functionals; however, the results in Table 8 indicate that the M06-L/aug-cc-pVTZ level of theory actually has better overall performance for the hydronium and hydroxide clusters than any of the MCCM, CBS, or MP2 methods. In addition, the M06-L/aug-cc-pVTZ method is the best of all 52 methods for the

TABLE 9: Reaction Energies (Kilocalories per Mole) for Association Reactions R13 to R28 Predicted by BMC-CCSD, G3SX(MP3), and M06-L/aug-cc-pVTZ

	BMC-CCSD	G3SX(MP3)	M06-L/aug-cc-pVTZ
R13	−75.98	−76.05	−76.54
R14	−42.97	−42.73	−42.20
R15	−19.70	−19.54	−19.53
R16	−101.26	−101.22	−101.26
R17	−68.25	−67.89	−66.92
R18	−44.98	−44.71	−44.25
R19	−25.28	−25.16	−24.72
R20	−29.51	−29.21	−28.41
R21	−84.59	−82.97	−87.36
R22	−84.40	−82.90	−86.74
R23	−58.04	−56.68	−60.13
R24	−57.85	−56.62	−59.52
R25	−36.38	−35.30	−38.04
R26	−36.19	−35.23	−37.43
R27	−17.54	−16.67	−19.26
R28	−17.35	−16.61	−18.64

TABLE 10: Reaction Energies (kcal/mol) for Neutralization Reactions R13 to R28 Predicted by BMC-CCSD, G3SX(MP3), and M06-L/aug-cc-pVTZ

	BMC-CCSD	G3SX(MP3)	M06-L/aug-cc-pVTZ
R45	−148.51	−147.86	−150.58
R46	−121.96	−121.58	−123.36
R47	−100.30	−100.19	−101.27
R48	−81.46	−81.57	−82.48
R49	−139.90	−140.95	−139.77
R50	−140.09	−141.01	−140.39
R51	−106.89	−107.62	−105.43
R52	−107.08	−107.69	−106.05
R53	−83.62	−84.44	−82.75
R54	−83.81	−84.50	−83.37
R55	−63.92	−64.89	−63.23
R56	−64.11	−64.96	−63.84
R57	−68.15	−68.93	−66.91
R58	−68.34	−69.00	−67.53
R59	−123.23	−122.70	−125.86
R60	−96.68	−96.41	−98.64
R61	−75.02	−75.03	−76.55
R62	−56.18	−56.40	−57.76
R63	−38.64	−39.73	−38.51
R64	−38.83	−39.80	−39.12

neutralization reactions and the fifth best method for the association reactions. Table 8 also shows that despite the relatively poor performance of M06-L for the pure water clusters (it ranks 14th out of 50 methods for the pure water clusters) it is tied for the third lowest scaled average (SA) with G3SX-(MP3), and its SA is only slightly higher than the best overall method, BMC-CCSD. If the water data is excluded, however, M06-L/aug-cc-pVTZ outperforms BMC-CCSD, G3SX, and CBS-QB3 (which are tied for second place) and is less expensive than G3SX.

As expected, we see that the MP2-based methods utilizing the correlation-consistent basis sets do very well for the pure water clusters, and they represent three of the five best methods for these binding reactions (BMC-CCSD is the third best behind MP2/aug′-cc-pVTZ and MP2/aug′-cc-pVQZ; CBS-APNO is the fourth best). However, when the MG3 and MG3S basis sets are used, MP2 does not perform well for pure water; in fact, the MP2/MG3 method is the second worst method and is better only than the MP2/MG3S method. Table 8 also shows that the three MP2 methods using the Dunning basis sets have the lowest error for the association reactions of the H_3O^+ and OH^- clusters, but when neutralization reactions are considered, all of the MP2 methods do very poorly. The best of the MP2 methods, MP2/MG3S, has a mean unsigned error of 2.51 kcal/mol and ranks 22rd out of 52 methods.

Of the fifteen MCCMs, the BMC-CCSD method performs the best; it is one of the top three methods for the neutralization reactions and for pure water clusters, and it has the eighth lowest error for the association reactions. BMC-CCSD also has the lowest mean unsigned error when all three categories (association, neutralization, and pure water) are considered, and as a result, it has the lowest scaled average of all MCCMs tested. As mentioned previously, if the pure water data is excluded, BMC-CCSD is tied with G3SX and CBS-QB3 for the second lowest scaled average, behind only M06-L/aug-cc-pVTZ. An additional advantage of BMC-CCSD is relatively low cost when compared with the other MCCM methods that perform well in Table 8. The BMC-CCSD method is a factor of 4 less expensive than G3SX(MP3) and CBS-QB3, a factor of 6 less costly than G3SX, and a factor of 29 less expensive than CBS-APNO, making it not only the most accurate of these methods, but also the most cost-effective.

The two CBS methods considered here show very different performance from each other. CBS-APNO and CBS-QB3 both do quite well for the association reactions (the two methods are ranked sixth and seventh, respectively). However, CBS-APNO does poorly for the neutralization reactions and has a MUE that is twice as large as the best method. CBS-QB3, on the other hand, is the seventh best method for these reactions. For the pure water data, we see that CBS-APNO does quite well and has the fourth lowest errors, while CBS-QB3 ranks 41st out of 52. Because of the very low error for the pure water clusters, CBS-APNO has the second lowest scaled average, but when the pure water data is excluded, it slips down to ninth. CBS-QB3 has a large scaled average, but when the pure water data is excluded, it is tied as the second best method.

The performance of B3LYP is relatively poor. It is not one of the top thirteen methods for any of the categories considered in this work, and on average, its errors are twice as large as the errors obtained with the best methods. As a result, the scaled averages for both the W42 and the IW28 databases are also twice as large as the three best methods. Additionally, we see that the best performance with the B3LYP functional comes with the 6-311+G(2d,2p) and 6-311+G(2df,2p) basis sets. The use of these basis sets gives a considerable savings over using the aug-cc-pVTZ basis set (nearly a factor of 10) while maintaining comparable quality in the results.

Looking at the performance of the local DFT methods, we find it clear that the two M06-L methods are the best. The M06-L/aug-cc-pVTZ method particularly dominates for the neutralization reactions where its error is half as large as the next best method, BPW91/6-311+G(2d,2p). The M06-L methods are also the two best methods for the association reactions. For pure water, M06-L/MG3S is tied for the second lowest mean unsigned error (of any DFT method) with PBE/aug-cc-pVTZ and has an MUE of 0.40 kcal/mol, while M06-L/aug-cc-pVTZ and PBE/aug-cc-pVDZ are tied with the third lowest MUE (0.47 kcal/mol).

Throughout Table 8, it is clear that a large basis set is needed in order for DFT (including the local functionals and B3LYP) to perform well for the hydronium and hydroxide clusters. The twelve best DFT methods for the association reactions and the top 13 DFT methods for the neutralization reaction use the aug-cc-pVDZ basis set or larger. For pure water, however, the M06-L, PBE, and PBE1W functionals need large basis sets (6-311+G(2df,2p), aug-cc-pVTZ, and 6-311+G(2d,2p), respectively) while the BLYP and B3LYP functionals do best with smaller basis sets (6-31+G(d,p) and 6-31(d,2p), respectively); these

TABLE 11: Mean Unsigned Deviations (Kilocalories per Mole) between the BMC-CCSD, G3SX(MP3), and M06-L/aug-cc-pVTZ Methods for the W78 Database

	R1−12 (12)	R13−28 (16)	R29−44 (16)	R45−64 (20)	water (14)	W (78)
BMC-CCSD−G3SX(MP3)	0.29	0.68	0.41	0.62	0.38	0.50
BMC-CCSD−M06-L[a]	0.67	1.25	1.14	1.04	0.52	0.95
G3SX(MP3)−M06-L	0.79	1.74	1.52	1.57	0.45	1.27

[a] Using the aug-cc-pVTZ basis set.

results are consistent with past work.[103] In the cases of BPW91 and PBELYP, neither functional does well for pure water with the two basis sets used here. PBELYP/aug-cc-pVTZ has an MUE of 1.05 kcal/mol, which is 5 times larger than the best DFT method, while PBELYP/6-311+G(2d,2p) has a mean unsigned error of 1.92 kcal/mol. The two BPW91 methods do even worse and are, in fact, the two worst methods for pure water with mean unsigned errors of 2.94 and 3.82 kcal/mol for the 6-311+G(2d,2p) and aug-cc-pVTZ basis sets, respectively.

It is also clear from Table 8 that use of the aug-cc-pVTZ basis set makes the DFT calculations considerably more expensive than for any other basis sets. On average, the cost increases by a factor of 3 as one goes from the 6-311+G(2df,-2p) basis set to the aug-cc-pVTZ basis set. Table 7 compares the number of primitive and contracted Gaussian basis functions for these two basis sets and shows that the aug-cc-pVTZ basis set has nearly twice as many basis functions as the 6-311+G-(2df,2p) basis set.

Since we are ultimately interested in calculating accurate reaction energies for clusters containing H_3O^+ and OH^- and are interested in methods with good overall performance, reaction energies for R13 to R28 and R45 to R64 were calculated at the M06-L/aug-cc-pVTZ, BMC-CCSD, and G3SX-(MP3) levels of theory. The association reaction energies predicted by the three methods for R13 to R28 are shown in Table 9. Examination of the eight association reactions containing H_3O^+ ions (R13 to R20) shows that, in general, M06-L predicts the smallest association energy, followed by G3SX-(MP3), followed by BMC-CCSD. The two lone exceptions are R13 and R16, which are both reactions involving the addition of water molecules to the hydronium ion. For the association reactions involving hydroxide ions (R21 to R 28), G3SX(MP3) predicts the smallest reaction energy, followed by BMC-CCSD and M06-L/aug-cc-pVTZ for all eight reactions.

A comparison for the neutralization reactions is given in Table 10. For the neutralization reactions, the results are a little more scattered, although in general the BMC−CCSD method seems to predict reaction energies that are midway between the other two methods; out of 20 reactions there are only 5 where this is not the case.

Table 11 shows the average mean deviations between the three methods. The results are broken down into five categories: association reactions with accurate Weizmann-1 energies and those without, neutralization reactions with accurate Weizmann-1 energies and those without, and the 13 water data from previous work[68,69] for which Weizmann-1 data are available; the final column is for the entire W78 data set. A comparison of the average deviations for the H_3O^+/OH^- reactions with Weizmann-1 energies and those without shows whether or not the trends of the methods stay the same as the larger ions are included. Overall, we see that the BMC-CCSD and G3SX(MP3) methods agree better with each other than either does with the M06-L/aug-cc-pVTZ method. Unfortunately, the average deviations more than double between the association reactions R1 to R12 and R13 to R38 and are one and a half times larger for R45 to R64 than for R29 to R44, despite the fact that the average reaction energies are smaller when the larger ions are included. This indicates that the performance of the methods may be a strong enough function of cluster size that there is no reliable way to draw conclusions about bulk work from the present smaller clusters to determine which is correct. For the water clusters without ions, the three methods agree beter than for any of the other categories.

4. Conclusions

We have tested a series of multicoefficient correlation methods, an extrapolated correlation method (CBS), the MP2 method, and B3LYP, and a variety of local DFT methods for their ability to reproduce Weizmann-1 association and neutralization energies for a data set of small hydronium and hydroxide clusters as well as binding energies for pure water clusters as large as the pentamer. We have found that the M06-L/aug-cc-pVTZ method is able to more accurately reproduce the Weizmann-1 results than any of the other 51 methods tested, including the MCCMs and CBS methods. The M06-L method has the lowest mean signed error for both the association and neutralization reactions, and its mean unsigned error for the water clusters without ions is only 0.37 kcal/mol higher than the best method. We also find that, while MP2 with a large basis set is able to do well for water clusters without ions and for the association reactions, it does very poorly for the neutralization reactions giving it a very large overall error. For the MCCM methods, BMC-CCSD, G3SX, and G3SX(MP3) are the best methods. In fact, if the data for pure water clusters are included in the total error, BMC-CCSD is slightly better than M06-L/aug-cc-pVTZ. G3SX and G3SX(MP3) are very similar for the association reactions; however, G3SX(MP3) is significantly less expensive. All other DFT methods have errors for the hydronium and hydroxide clusters that are twice as large as M06-L. For the larger clusters, we find that the deviations between BMC-CCSD, G3SC(MP3), and M06-L/aug-cc-pVTZ are larger even though the average magnitude of the reaction energies are smaller. As a result, there is no way to determine which of these three most accurate methods is more reliable than the others, and all three may be recommended for future studies. One should note, however, that they have different costs, as shown in the final column of Table 8.

Acknowledgment. This work was supported in part by the National Science Foundation under Grants ITR-0428774 and CHE-0704974.

Supporting Information Available: Cartesian coordinates for the hydronium- and hydroxide-containing clusters and complete versions of Table 8 and Table 11 showing mean signed and root-mean-squared errors. This material is available free of charge via the Internet at http://pubs.acs.org.

References and Notes

(1) Bernal, J. D.; Fowler, R. H. *J. Chem. Phys.* **1933**, *1*, 515.
(2) Grotthuss, C. J. T. *Ann. Chim. (Paris*), **1806**, *58*, 54.

(3) Wicke, E.; Eigen, M.; Ackermann, T. *Z. Phys. Chem. (Munich*) **1954**, *1*, 340.
(4) Eigen, M. *Angew. Chem., Int. Ed. Engl.* **1964**, *3*, 1.
(5) Zundel, G.; Metzger, H. *Z. Phys. Chem. (Munich*) **1968**, *58*, 225.
(6) Tuckerman, M. E.; Marx, D.; Parrinello, M. *Nature* **2002**, *417*, 925.
(7) Laasonen, K.; Klein, M. L. *J. Phys. Chem.* **1994**, *98*, 10079.
(8) Xie, Y.; Remington, R. B.; Scaefer, H. F., III *J. Chem. Phys.* **1994**, *101*, 4878.
(9) Hodges, M. P.; Stone, A. J. *J. Chem. Phys.* **1999**, *110*, 6766.
(10) Pliego, J. R.; Riveros, J. M. *J. Chem. Phys.* **2000**, *112*, 4045.
(11) Mejías, J. A.; Lago, S. *J. Chem. Phys.* **2000**, *113*, 7306.
(12) Masamura, M. *Chem. Phys. Lett.* **2001**, *339*, 279.
(13) Kim, Y.; Kim, Y. *Chem. Phys. Lett.* **2002**, *362*, 419.
(14) Miani, A.; Beddoni, A.; Personen, J.; Halonen, L. *Chem. Phys. Lett.* **2002**, *363*, 52.
(15) Turki, N.; Milet, Ouamerali, A., O.; Moszynski, R.; Kockanski, E. *THEOCHEM* **2002**, *577*, 239.
(16) Lee, H. M.; Tarkeshwar, P.; Kim, K. S. *J. Chem. Phys.* **2004**, *121*, 4657.
(17) Headrick, J. M.; Diken, E. G.; Walters, R. S.; Hammer, N. I.; Christie, R. A.; Cui, J.; Myshakin, E. M.; Duncan, M. A.; Johnson, M. A.; Jordan, K. D. *Science* **2005**, *308*, 1765.
(18) Huang, X.; Braams, B. J.; Bowman, J. M. *J. Chem. Phys.* **2005**, *122*, 44308.
(19) James, T.; Wales, D. J. *J. Chem. Phys.* **2005**, *122*, 134306.
(20) Picard, F. C., IV; Pokon, E. K.; Liptak, M. D.; Shields, G. C. *J. Chem. Phys.* **2005**, *122*, 24302.
(21) Svozil, D.; Jungwirth, P. *J. Phys. Chem. A* **2006**, *110*, 9194.
(22) Tuckerman, M.; Laasonen, K.; Sprik, M. *J. Chem. Phys.* **1995**, *103*, 150.
(23) Geissler, P. L.; Dellago, C.; Chandler, D.; Hutter, J.; Parrinello, M. *Science* **2001**, *291*, 2121.
(24) Kornyshev, A. A.; Kuznetsov, A. M.; Spohr, E.; Ulstrup, J. *J. Phys. Chem. B* **2003**, *107*, 3351.
(25) Asthagiri, D.; Pratt, L. R.; Kress, J. D.; Gomez, M. A. *Proc. Natl. Acad. Sci. U.S.A.* **2004**, *101*, 7229.
(26) Campo, M. G.; Grigera, J. R. *Mol. Sim.* **2004**, *30*, 537.
(27) Asthagiri, D.; Pratt, L. R.; Kress, J. D. *Proc. Natl. Acad. Sci. U.S.A.* **2005**, *102*, 6704.
(28) Brancato, G.; Tuckerman, M. E. *J. Chem. Phys.* **2005**, *122*, 224507.
(29) Imberti, S.; Botti, A.; Bruni, F.; Cappa, G.; Ricci, M. A.; Soper, A. K. *J. Chem. Phys.* **2005**, *122*, 194509.
(30) Izvekov, S.; Voth, G. A. *J. Chem. Phys.* **2005**, *123*, 44505.
(31) Wang, F.; Voth, G. A. *J. Chem. Phys.* **2005**, *122*, 144105.
(32) Han, J.; Zhou, X.; Liu, H. *J. Power Sources* **2006**, *161*, 1420.
(33) Tuckerman, M. E.; Chandra, A.; Marx, D. *Acc. Chem. Res.* **2006**, *39*, 151.
(34) Voth, G. A. *Acc. Chem. Res.* **2006**, *39*, 143.
(35) Kobayashi, C.; Saito, S.; Ohmine, I. *J. Chem. Phys.* **2000**, *113*, 9090.
(36) Kobayashi, C.; Saito, S.; Ohmine, I. *J. Chem. Phys.* **2001**, *115*, 4742.
(37) Cizek, J. *Adv. Chem. Phys.* **1969**, *14*, 35.
(38) Purvis, G. D.; Bartlett, R. J. *J. Chem. Phys.* **1982**, *76*, 1910.
(39) Raghavachari, K.; Trucks, G. W.; Pople, J. A.; Head-Gordon, M. *Chem. Phys. Lett.* **1989**, *157*, 479.
(40) Pople, J. A.; Head-Gordon, M.; Fox, D. J.; Raghavachari, K.; Curtiss, L. A. *J. Chem. Phys.* **1989**, *90*, 5622.
(41) Curtiss, L. A.; Jones, C.; Trucks, G. W.; Ragavachari, K.; Pople, J. A. *J. Chem. Phys.* **1990**, *93*, 2537.
(42) Curtiss, L. A.; Raghavachari, K.; Trucks, G. W.; Pople, J. A. *J. Chem. Phys.* **1991**, *94*, 7221.
(43) Curtiss, L. A.; Raghavachari, K.; Redfern, P. C.; Rassolov, V.; Pople, J. A. *J. Chem. Phys.* **1998**, *019*, 7764.
(44) Raghavachari, K.; Curtiss, L. A. In *Theory and Applications of Computational Chemistry: The First Forty Years;* Dykstra, C., Frenking, G., Kim, K., Scuseria, G., Eds.; Elsevier: Amsterdam, 2005; p 785.
(45) Nyden, M. R.; Petersson, G. A. *J. Chem. Phys.* **1981**, *75*, 1843.
(46) Petersson, G. A.; Bennett, A.; Tensfeldt, T. G.; Al-Laham, M. A.; Shirley, W. A.; Mantzaris, J. *J. Chem. Phys.* **1988**, *89*, 2193.
(47) Petersson, G. A.; Al-Laham, M. A. *J. Chem. Phys.* **1991**, *94*, 6081.
(48) Petersson, G. A.; Tensfeldt, T. G.; Montgomery, J. A., Jr. *J. Chem. Phys.* **1991**, *94*, 6091.
(49) Montgomery, J. A., Jr.; Ochterski, J. W.; Petersson, G. A. *J. Chem. Phys.* **1994**, *101*, 5900.
(50) Ochterski, J. W.; Petersson, G. A.; Montgomery, J. A., Jr. *J. Chem. Phys.* **1996**, *104*, 2598.
(51) Montgomery, J. A., Jr.; Frisch, M. J.; Ochterski, J. W.; Petersson, G. A. *J. Chem. Phys.* **1999**, *110*, 2822.
(52) Montgomery, J. A., Jr.; Frisch, M. J.; Ochterski, J. W.; Petersson, G. A. *J. Chem. Phys.* **2000**, *112*, 6532.
(53) Fast, P. L.; Corchado, J.; Sanchez, M. L.; Truhlar, D. G. *J. Phys. Chem. A* **1999**, *103*, 3139.
(54) Fast, P. L.; Corchado, J.; Sanchez, M. L.; Trucks, G. W. *J. Phys. Chem. A* **1999**, *103*, 5129.
(55) Fast, P. L.; Sanchez, M. L.; Truhlar, D. G. *Chem. Phys. Lett.* **1999**, *306*, 407.
(56) Fast, P. L.; Sanchez, M. L.; Corchado, J.; Truhlar, D. G. *J. Chem. Phys.* **1999**, *110*, 11679.
(57) Tratz, C. M.; Fast, P. L.; Truhlar, D. G. *Phys. Chem. Commun.* **1999**, *2*, 70.
(58) Lynch, B. J.; Truhlar, D. G. *J. Phys. Chem. A* **2003**, *107*, 3898.
(59) Zhao, Y.; Lynch, B. L.; Truhlar, D. G. *Phys. Chem. Chem. Phys.* **2007**, *7*, 43.
(60) Lynch, B. J.; Truhlar, D. G. In *Electron Correlation Methodology*; Wilson, A. K., Peterson, K. A., Eds.; ACS Symposium Series 958; Oxford University Press: New York, 2007; pp 153−167.
(61) Curtiss, L. A.; Redfern, P. C.; Rassolov, V.; Kedziora, G.; Pople, J. A. *J. Chem. Phys.* **2001**, *114*, 108.
(62) Hashimoto, T.; Hiwatari, Y. *Mol. Simul.* **1998**, *21*, 239.
(63) McGrath, M. J.; Siepmann, J. I.; Kuo, I.-F. W.; Mundy, C. J.; VandeVondele, J.; Hutter, J.; Mohamed, F.; Krack, M. *J. Phys. Chem. A* **2006**, *110*, 640.
(64) Kuo, I.-F. W.; Mundy, C. J.; Eggimann, B. L.; McGrath, M. J.; Siepmann, J. I.; Chen, B.; Vieceli, J.; Tobias, D. J. *J. Phys. Chem. B* **2006**, *110*, 3738.
(65) Becke, A. D. *Phys. Rev. A* **1988**, *38*, 3098.
(66) Lee, C.; Yang, W.; Parr, R. G. *Phys. Rev. B* **1988**, *37*, 785.
(67) Perdew, J. P.; Burke, K.; Ernzerhof, M. *Phys. Rev. Lett.* **1996**, *77*, 3865.
(68) Dahlke, E. E.; Truhlar, D. G. *J. Phys. Chem. B* **2006**, *109*, 15677.
(69) Dahlke, E. E.; Truhlar, D. G. *J. Phys. Chem. B* **2006**, *110*, 10595.
(70) Islam, M. M.; Maslyuk, V. V.; Bredow, T.; Minot, C. *J. Phys. Chem. B* **2005**, *109*, 13597.
(71) VandeVondele, J.; Mohamed, F.; Krack, M.; Hutter, J.; Sprik, M.; Parrinello, M. *J. Chem. Phys.* **2005**, *122*, 14515.
(72) Paier, J.; Hirschl, R.; Marsman, M.; Kresse, G. *J. Chem. Phys.* **2005**, *122*, 234102.
(73) Cinquini, F.; Giordano, L.; Pacchioni, G.; Ferrari, A. M.; Pisani, C.; Roetti, C. *Phys. Rev. B* **2006**, *74*, 165403.
(74) Paier, J.; Marsman, M.; Hummer, K.; Kresse, G.; Gerber, I. C.; Ángyán, J. G. *J. Chem. Phys.* **2006**, *124*, 154709.
(75) Paier, J.; Marsman, M.; Hummer, K.; Kresse, G.; Gerber, I. C.; Ángyán, J. G. *J. Chem. Phys.* **2006**, *125*, 249901.
(76) Todorova, T.; Seitsonen, A. P.; Hutter, J.; Kuo, I.-F. W.; Mundy, C. J. *J. Phys. Chem. B* **2006**, *110*, 3685.
(77) Tran, F.; Blaha, P.; Schwarz, K.; Novák, P. *Phys. Rev. B* **2006**, *74*, 155108.
(78) Labat, F.; Baranek, P.; Domain, C.; Minot, C.; Adamo, C. *J. Chem. Phys.* **2007**, *126*, 154703.
(79) Paier, J.; Marsman, M.; Kresse, G. *J. Chem. Phys.* **2007**, *127*, 24103.
(80) Pople, J. A.; Head-Gordon, M.; Raghavachari, K. *J. Chem. Phys.* **1987**, *87*, 5968.
(81) Lynch, B. J.; Zhao, Y.; Truhlar, D. G. *J. Phys. Chem. A* **2003**, *107*, 1384.
(82) Krishnan, R.; Binkley, J. S.; Seeger, R.; Pople, J. A. *J. Chem. Phys.* **1980**, *72*, 650.
(83) Clark, T.; Chandrasekhar, J.; Spitznagel, G. W.; Schleyer, P. v. R. *J. Comput. Chem.* **1983**, *4*, 294.
(84) Møller, C.; Plesset, M. S. *Phys. Rev.* **1934**, *46*, 618.
(85) Lynch, B. L.; Zhao, Y.; Truhlar, D. G. *J. Phys. Chem. A* **2005**, *109*, 1643.
(86) Martin, J. M. L.; Oliveira, G. d. *J. Chem. Phys.* **1999**, *111*, 1843.
(87) Woon, D. E.; Dunning, T. H., Jr. *J. Chem. Phys.* **1993**, *98*, 1358.
(88) Kendall, R. A.; Dunning, T. H., Jr.; Harrison, R. J. *J. Chem. Phys.* **1995**, *96*, 6796.
(89) Dunning, T. H. *J. Chem. Phys.* **1989**, *90*, 1007.
(90) Zhao, Y.; Truhlar, D. G. *MLGAUSS-version 1.0*, University of Minnesota: Minneapolis, 2005.
(91) Frisch, M. J.; Trucks, G. W.; Schlegel, H. B.; Robb, G. E. S. M. A.; Cheeseman, J. R.; Montgomery, J. A., Jr; Vreven, T.; Kudin, K. N.; Burant, J. C.; Millam, J. M.; Iyengar, S. S.; Tomasi, J.; Barone, V.; Mennucci, B.; Cossi, M.; Scalmani, G.; Rega, N.; Petersson, G. A.; Nakatsuji, H.; Hada, M.; Ehara, M.; Toyota, K.; Fukuda, R.; Hasegawa, J.; Ishida, M.; Nakajima, T.; Honda, Y.; Kitao, O.; Nakai, H.; Klene, M.; Li, X.; Knox, J. E.; Hratchian, H. P.; Cross, J. B.; Adamo, C.; Jaramillo, J.; Gomperts, R.; Stratmann, R. E.; Yazyev, O.; Austin, A. J.; Cammi, R.; Pomelli, C.; Ochterski, J. W.; Ayala, P. Y.; Morokuma, K.; Voth, G. A.; Salvador, P.; Dannenberg, J. J.; Zakrzewski, V. G.; Dapprich, S.; Daniels, A. D.; Strain, M. C.; Farkas, O.; Malick, D. K.; Rabuck, A. D.; Raghavachari, K.; Foresman, J. B.; Ortiz, J. V.; Cui, Q.; Baboul, A. G.; S. Clifford; Cioslowski, J.; Stefanov, B. B.; Liu, G.; Liashenko, A.; P. Piskorz; Komaromi, I.; Martin, R. L.; Fox, D. J.; Keith, T.; M. A. Al-Laham; Peng, C. Y.; Nanayakkara, A.; Challacombe, M.; P. M. W. Gill; Johnson, B.; Chen, W.; Wong, M. W.; Gonzalez, C.; Pople, J. A. *Gaussian 03*, Revision c01; Gaussian Inc.: Wallingford, CT, 2004.

(92) Becke, A. D. *J. Chem. Phys.* **1993**, *98*, 5648.
(93) Stephens, P. J.; Devlin, F. J.; Chabalowski, C. F.; Frisch, M. J. *J. Phys. Chem.* **1994**, *98*, 11623.
(94) Perdew, J. P. In *Electronic Structure of Solids '91*; Ziesche, P., Esching, H., Eds.; Akademie Verlag: Berlin, 1991; p 11.
(95) Zhao, Y.; Truhlar, D. G. *J. Chem. Phys.* **2006**, *125*, 194101.
(96) Kuo, J.-L.; Klein, M. L. *J. Phys. Chem. B* **2004**, *108*, 19634.
(97) Umemoto, K.; Wentzcovich, R. M. *Phys. Rev. B* **2004**, *69*, 180103.
(98) Umemoto, K.; Wentzcovich, R. M.; Baroni, S.; Gironcoli, S. d. *Phys. Rev. Lett.* **2004**, *92*, 105502.
(99) Knight, C.; Singer, S. J.; Kuo, J.-L.; Hirsch, T. K.; Ojamäe, L.; Klein, M. L. *Phys. Rev. E* **2006**, *73*, 53116.
(100) Kuo, I.-F. W.; Mundy, C. J.; McGrath, M. J.; Siepmann, J. I. *J. Chem. Theory Comput.* **2006**, *2*, 1274.
(101) McGrath, M. J.; Siepmann, I. J.; Kuo, I.-F. W.; Mundy, C. J. *Mol. Phys.* **2006**, *104*, 3619.
(102) Hehre, W. J.; Radom, L.; Schleyer, P. v. R.; Pople, J. A. In *Ab Initio Molecular Orbital Theory;* Wiley: New York, 1986; p 576.
(103) Csonka, G. I.; Ruzsinszky, A.; Perdew, J. P. *J. Phys. Chem. B* **2005**, *109*, 21471.
(104) Zhao, Y.; Truhlar, D. G. *Theor. Chem. Acc.* Published on-line at http://dx.doi.org/10.1007/S00214-007-0310-x.
(105) Zhao, Y.; Truhlar, D. G. *MN-GFM: Minnesota Gaussian Functional Module- version 2.0.1*; University of Minnesota: Minneapolis, 2006.